Molecular Crystals and Liquid Crystals Science and Technology. Section A. Molecular Crystals and Liquid Crystals

Publication details, including instructions for authors and subscription information:
http://www.tandfonline.com/loi/gmcl19

Theory of Electroconvection for the Gourmet

L. Kramer [a], B. Dressel [a], H. Zhao [a] & W. Pesch [a]

[a] Physikalisches Institut, Universität Bayreuth, D-95440, Bayreuth, Germany

Version of record first published: 24 Sep 2006

To cite this article: L. Kramer, B. Dressel, H. Zhao & W. Pesch (2001): Theory of Electroconvection for the Gourmet, Molecular Crystals and Liquid Crystals Science and Technology. Section A. Molecular Crystals and Liquid Crystals, 364:1, 101-110

To link to this article: http://dx.doi.org/10.1080/10587250108024980

Mol. Cryst. and Liq. Cryst., 2001, Vol. 364, pp. 101-110
Reprints available directly from the publisher
Photocopying permitted by license only

Theory of Electroconvection for the Gourmet

L. KRAMER, B. DRESSEL, H. ZHAO and W. PESCH

Physikalisches Institut, Universität Bayreuth, D-95440 Bayreuth, Germany

In the last years the understanding of electroconvection in nematics in the nonlinear regime has benefitted considerably from the use of reduced descriptions that can be obtained largely from a phenomenological approach. Close connection with hydrodynamic theory and experiments is essential.

Keywords: electroconvection; pattern formation in nematics; nonlinear theory

INTRODUCTION

The description of a complex phenomenon like electroconvection in nematics has to start from hydrodynamic theory (for reviews see [1, 2]). One has the usual nematodynamic equations supplemented by an electric part, which consists of the charge conservation equation with Poisson's law. The material is described by an anisotropic dielectric tensor, and, in the Helfrich "standard model" (SM), by an ohmic conductivity tensor. In the Navier-Stokes equation the Maxwell stress tensor has to be included. The full linear stability analysis of the SM is nowadays feasible, even with the inclusion of the flexoeffect (which has limited influence under the usual ac driving).

The SM describes all measured effects, like normal and oblique rolls at threshold, conduction and dielectric destabilization depending on frequency ω (see Fig. 1a for a sketch). To describe the observed traveling rolls [3], a generalization, the "weak electrolyte model" (WEM), has been developed. Here an additional dynamic process is

included by considering two species of mobile ions which arise in a (slow) dissociation-recombination reaction [4, 5].

The first task of nonlinear theory is to describe the saturation of the pattern evolving from the linear modes in the spirit of a (time-dependent) Landau theory [6]. In the oblique-roll regime a superposition of zig and zag rolls leading to rectangular structures is in principle possible. Next, slow spatial modulations of the ideal periodic pattern with wave vector $\mathbf{q}_c$ are included by introducing a slowly varying complex amplitude A such that the pattern is described by the real part of $A(\mathbf{x})exp(i\mathbf{q}_c\mathbf{x})$. The generic amplitude equation for anisotropic systems in the range of static normal rolls is the real Ginzburg-Landau equation [7, 8, 6]

$$\tau\partial_t A = \left(\epsilon - g|A|^2 + \xi_1^2\partial_x^2 + \xi_2^2\partial_y^2\right) A, \tag{1}$$

where $\epsilon = (V^2 - V_c^2)/V_c^2$, with the critical voltage V_c, is the reduced control parameter. g (> 0 in the SM) describes the nonlinear saturation and $\xi_{1,2}$ represent the coherence lengths. Generalization to the neighbourhood of the Lifshitz point ω_L, which separates the normal ($\omega > \omega_L$) from the oblique roll regime, is possible [7]. Deep inside the oblique-roll range one has to use two coupled equations. The coefficients of the amplitude equations were calculated from the SM in [6] (without flexoeffect). The Ginzburg-Landau equations can be used in particular to study the stable wavevector band (the wavenumber and the orientation can be changed to some extent without loosing stability) and the structure and dynamics of dislocations, in good agreement with experiments [9].

In the framework of the WEM the Hopf bifurcation to travelling rolls is supercritical. Then one has the complex Ginzburg-Landau equation (actually two or four such coupled equations for the counter-propagating, and possibly oblique, roll systems [10]) to describe the weakly nonlinear behaviour [5]. The stationary bifurcation near the crossover to travelling rolls is typically subcritical. The resulting small hysteresis has been measured in various materials [11, 12, 4]. Particularly interesting scenarios involving extended spatio-temporal chaos at onset [13] and subcritically arising localized structures ("worms") [14] have been found in the material Merck I52.

The former can be understood on the basis of two coupled complex Ginzburg-Landau equations describing zig and zag rolls travelling in the same direction [15]. A phenomenological model has been proposed to describe the worms [16]. Well inside the nonlinear regime WEM effects are presumably negligible because the velocity field tends to level out gradients in the density of the charge carriers. Thus any extended nonlinear analysis has been considered within the SM.

EXTENDED NONLINEAR REGIME

To extend the range of validity of the above description various finite$-\epsilon$ corrections have been taken into account [17]. In particular the curvature of rolls is known to induce a so called mean flow. In the presence of 2D lateral spatial variations (3D on the hydrodynamic level) the mean flow cannot be fully eliminated due to the singular structure of its spatial dependence. Thus, one is left with an additional (static) equation. The analysis showed that, at least near to the transition to oblique rolls, normal rolls are destabilized with increasing ϵ by a zigzag (or undulatory) instability at ϵ_{ZZ} as found in experiments [18].

A full numerical Galerkin calculation confirmed this result and extended it to larger ϵ and frequencies [19, 20]. Surprisingly, at frequencies above some value $\omega_{AR} > \omega_L$ (to the right of $C2$ in Fig. 1a destabilization of normal rolls occurs at $\epsilon = \epsilon_{AR}$ via a spatially homogeneous (in the plane of the layer) mode involving a twist of the director. The mode is the analog of that which destabilizes the basic state in a twist Fréedericksz transition (magnetic field in the y direction). The instability signalizes a (continuous) pitchfork bifurcation from normal to "abnormal rolls" (ARs) where the director attains such a twist deformation, either to the left or to the right. Interestingly one has restabilization of ARs for $\omega < \omega_{AR}$ above ϵ_{ARst}. This line will be discussed in greater detail subsequently. At larger ϵ the ARs destabilize either via a long-wave skewed-varicose instability (SV) (here the modulation wave vector of the destabilizing mode is at an oblique angle), or, at smaller frequency, via a short-wave

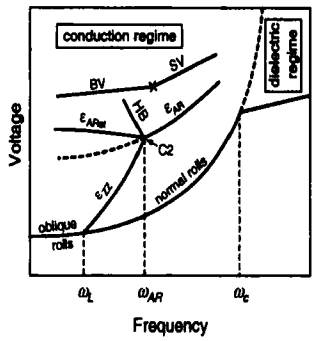

Fig.1a. Schematic stability diagram for planar EC. Convection sets in above the lowest solid curves. For the secondary bifurcations, see text.

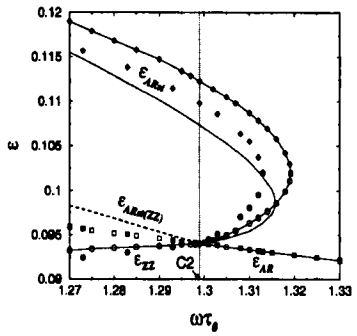

Fig.1b. Blow-up of the vicinity of the C2-point for the material MBBA (τ_0: charge relaxation time) showing the modification of ϵ_{ARst} by skewed-varicose modulations. For details, see text.

skewed-varicose instability. This is also called a bimodal varicose instability (BV) [21, 20], because it indicates the transition to a bimodal state composed of the superposition of two roll systems with different orientation.

When one extends this diagram to oblique rolls (wavevector $\mathbf{q} = (q, p)$), the AR bifurcation becomes imperfect (smooth), since in oblique rolls the left-right symmetry is already broken. Also, the destabilization is shifted upward and restabilization downward, so that the curves meet at some value $P_m(\omega)$ (with vertical slope) [19]. Thus one has an unstable bubble in the $\epsilon - P$ plane which is bounded from below by ϵ_{ZZ}, and from above by ϵ_{ARst} [22, 23]. Consequently there is a very interesting codimension-2 (C2) point at $\omega_{AR}, \epsilon_{AR}$.

The reason why ARs had escaped the notice of experimentalists is that in planarly aligned cells and with the ordinary visualization (at most one polarizer in x direction) they cannot be distinguished from NRs. For homeotropic alignment this is different, and there the signature of ARs had indeed been observed before [24]. Indirect evidence comes from the observation of domain walls between the two variants of ARs [19]. Meanwhile direct evidence has been

obtained from measurements of the ellipticity of the light induced by ARs [25, 26]. In these measurements also the ZZ instability, together with the restabilization line, could be identified. Apparently the rather small width of the system in the x direction, which allowed for 12 roll pairs, stabilized the ZZ structures, which appear above the instability, otherwise they are unstable against coarsening. Interestingly, another line at ϵ_{HB} was found, which lies above ϵ_{ARst} and also goes through the C2 point: whereas the angle of the ZZ structures first increases with ϵ when ϵ_{ZZ} is crossed, it subsequently decreases again, becoming zero at ϵ_{HB}. Then one is left with ARs with domain walls, because the different orientations in the ZZs induce different variants of ARs. The domain walls quickly annihilate and there remains a single AR domain. When one now decreases ϵ, a massive hysteresis occurs: the ARs persist down to ϵ_{ARst}. Then there is a discontinuous transition to the ZZ branch.

These features can be understood in terms of a simple, phenomenological description of the AR bifurcation [25, 23]. The two active modes involved are the twist mode, characterized by an angle ϕ, and the phase of the modulations of the roll pattern θ. The equations are

$$\begin{aligned} \partial_t \phi &= (\mu - g\phi^2)\phi + (K_1\partial_x^2 + K_2\partial_y^2)\phi - \gamma\partial_y\theta, \\ \partial_t \theta &= (D_1\partial_x^2 + D_2\partial_y^2)\theta - (\nu + h\phi^2)\partial_y\phi, \end{aligned} \tag{2}$$

The control parameters μ and ν are to be associated with $\epsilon - \epsilon_{AR}$ and $\omega - \omega_{AR}$. The coupling terms are obtained from symmetry considerations. The term proportional to h is included because ν goes through zero. (A similar term in the ϕ equation would allow to include destabilization of ARs at larger values of μ.) This model contains all the features described above. The slopes of the different lines are easily expressed in terms of the parameters of the model. In particular, for $\nu < 0$, the ZZ instability of NRs at $\mu = (\gamma/D_2)\nu$ preempts the AR instability and ARs exhibit the observed restabilization. At the HB line there is a heteroclinic connection between ZZ solutions and NRs. Above the HB line domain walls that are not parallel to the rolls move spontaneously [23].

This description is well-founded when only modulations along y

occur, like in the ZZ instability and in ZZ solutions. In order to describe y and x variations, one has to include in particular singular mean flow by adding a term $-S_1\partial_y G$ on the rhs of the $\theta-$equation where G satisfies the equation $\nu_a\partial_x^2 G+\nu_b\partial_y^2 G+d_1\partial_x^2\phi+d_3\phi\partial_x\partial_y\phi=0$. This changes the restabilization from a ZZ into a skewed-varicose instability and moves it upward. With parameters calculated from hydrodynamics for MBBA the effect is particularly strong near the C2 point where in fact a "nose" develops, see Fig. 1b (solid curve without symbols). Also included is the restabilization line as obtained from full Galerkin calculations (symbols only) [27]. It would be interesting to identify the "nose" experimentally (the experiments in [25, 26] were presumably not accurate enough).

The reduced descriptions (1) and (2) are mutually exclusive: they represent normal-form type models of the primary and the secondary bifurcations, respectively. One can combine them by replacing in (2) the phase of the pattern by its complex amplitude. The simplest version of such equations

$$\begin{aligned}\tau\partial_t A &= \left[\epsilon - g|A|^2+\xi_1^2\partial_x^2+\xi_2^2(\partial_y^2-2iC_1q_c\phi\partial_y-C_2q_c^2\phi^2-i\nu\,\partial_y\phi)\right]A,\\ \partial_t\phi &= G(iq_cA^*(\partial_y-iq_c\phi)A+c.c)-T\phi+(K_1\partial_x^2+K_2\partial_y^2)\phi. \qquad (3)\end{aligned}$$

is quantitatively valid when the secondary bifurcation is near to the primary one [28].

Such a situation occurs naturally in homeotropically aligned systems in materials with manifestly negative dielectric anisotropy, where one first has a bend Fréedericksz transition through which the director acquires a planar component (planar director **c**). The transition to convection occurring at higher voltage is in many ways similar to that in planar cells, except that the preferred axis (the **c** director) is not externally fixed. The Goldstone mode related to rotation of the **c** director, which is here the analog of the twist mode, is now undamped ($T=0$ in Eqs.(3), which means that the AR bifurcation coincides with the primary one. In this case one also has from overall rotation invariance $C_1=C_2=1$ [29, 28](in general $1\geq C_2^2>C_1$). The first term in the $\phi-$equation expresses the "abnormal torque" on the **c** director ($G>0$!), which arises at second order in the

convection amplitude. For $T = 0$ all roll solutions are unstable. In simulations ϕ grows without bounds (for $C_1 = C_2 = 1$!), and then a globally invariant generalization of these equations must be used, which exhibit dynamic disorder ("soft-mode turbulence") [29, 28], which is essentially what is found experimentally [24, 30, 31, 32].

The linear damping $\sim T$ appears in the presence of effects that break rotation invariance, like an additional planar magnetic field (then $T \approx \chi_a H^2$). Then one has a situation which is in some ways similar to the planar case. In planar systems, on the other hand, the AR bifurcation can be shifted downward by applying an additional (destabilizing) magnetic field in the y direction. Then $T \approx \chi_a(H_F^2 - H^2)$ so that T, and therefore also ϵ_{AR}, tends to zero for $H \to H_F$. In that situation Eqs.(3) apply quantitatively (now $1 \geq C_2^2 > C_1$). In simulations ϕ remains bounded even for $T = 0$, in contrast to the case $C_1 = C_2 = 1$.

For $T > 0$ Eqs.(3) describe NRs at band center ($|A| = \sqrt{\epsilon/g}$, $\phi = 0$), which are stable against homogeneous ϕ perturbations for $\epsilon < \epsilon_{AR} = T/(2G)$ and against ZZ fluctuations for $\epsilon < \epsilon_{ZZ} = \epsilon_{AR}/(1-\nu)$. A quantitative comparison of the pitchfork bifurcation to ARs $A = \sqrt{\epsilon_{AR}/g}$, $\phi = \sqrt{(\epsilon - \epsilon_{AR}/(\xi_1 q_c)}$ with experiment has been made in a homeotropic cell [33].

For negative ν one has a restabilization curve which passes through the C2 point with slope $d\epsilon/d\nu = -1/(2(1 - C_1))$ and saturates for $\nu \to -\infty$ at $\epsilon_\infty = C_2/(2C_1 + C_2)$. Destabilization of ARs towards increasing ϵ is also captured. For negative values of ν there is a short-wave instability merging with a long-wave instability curve at some positive ν. For $\nu \to \infty$ the instability curve tends to ϵ_∞ from above. Thus the scenario is qualitatively as in Fig.1a. For C_1, $C_2 \to 1$ the scenario degenerates such that there is in effect no restabilization (actually for $\nu < 0$ there is restabilization at $\epsilon = 3/2\epsilon_{AR}$, but at the same line the short-wave destabilization sets in [28]) and destabilization of ARs for $\nu > 0$ occurs at $\epsilon = 3/2\epsilon_{AR}$.

In the range of stable ARs the equations describe interesting defect scenarios. For ϵ above the stable range one has defect chaotic states. For $\epsilon \gg \epsilon_{AR}$ (this can be achieved for any positive value of ϵ by choosing T (> 0) sufficiently small) one has a spontaneous

ordering of defects along periodically arranged lines along y, which appears to explain the most common types of chevrons observed in the dielectric range of planarly aligned cells [34]. The theory is indeed applicable to the dielectric range because here the orienting effects of the boundaries can be considered as small perturbations [35], which is consistent with experiments [36, 37]. The prediction that chevrons should occur in homeotropic systems also in the conduction range has been verified [30, 32]. For $1 \geq C_2^2 > C_1$ one also has a new type of static chevrons (at larger ϵ) [38].

When ϵ_{AR} is not sufficiently small, as is the case for planar systems without additional magnetic field, corrections have to be included, which in particular involve mean flow. This has been carried out for the case with modulations only in the y direction [20] (as mentioned before, mean flow can then be eliminated). Otherwise the equations become somewhat tedious, so we will not write them out here. In Fig. 1b the restabilization line (with the "nose") is included as obtained from the extended equations (solid curve with symbols). We intend to study complex patterns with these equations.

CONCLUSION

We could sketch here only some rather basic results while work on various detailed aspects is still in progress. There is hope that phenomena like the "wide domains" [39, 40, 41] (or "prechevrons" [32, 42]), which seemingly arise in a primary instability, but can be understood only as a secondary bifurcation (they resemble the static chevrons mentioned before), will eventually be understood. Possibly the instability of drift-recombination induced boundary layers as described by the WEM [43] can lead to convection at the boundaries as observed many years ago [44]. These effects would presumably persist in the isotropic phase which would be consistent with old [45] and new results [42].

References

[1] L. Kramer and W. Pesch, Annu. Rev. Fluid Mech. **27**, 515 (1995); W. Pesch and U. Behn in "Evolution of Spontaneous Structures in Dissipative Continuous Systems" F. H. Busse and S. C. Müller, eds., Springer, 1998.

[2] A. Buka and L. Kramer, *Pattern formation in liquid crystals* (Springer-Verlag, New-York, 1996).

[3] S. Kai and K. Hirakawa, Prog. Theor. Phys. Suppl. **14**, 212 (1978); A. Joets and R. Ribotta, Phys. Rev. Lett. **60**, 2164 (1988); I. Rehberg, S. Rasenat, and V. Steinberg, Phys. Rev. Lett. **62**, 756 (1989); M. Treiber, N. Eber, A. Buka, and L. Kramer, J. Phys. France II **7**, 649 (1997).
[4] M. Dennin, M. Treiber, L. Kramer, G. Ahlers, and D. Cannell, Phys. Rev. Lett. **76**, 319 (1996).
[5] M. Treiber and L. Kramer, Phys. Rev. E **58**, 1973 (1998).
[6] E. Bodenschatz, W. Zimmermann, and L. Kramer, J. Phys.(Paris) **49**, 1875 (1988).
[7] W. Pesch and L. Kramer, Z. Phys. B **63**, 121 (1986).
[8] See the contribution of W. Pesch and L. Kramer in [2].
[9] E. Bodenschatz, W. Pesch and L. Kramer, Physica D **32**, 135 (1988); L. Kramer, E. Bodenschatz and W. Pesch, Phys. Rev. Lett. **64**, 2588 (1990); E. Bodenschatz, A. Weber, and L. Kramer, J. Stat. Phys. **64**, 1007 (1991).
[10] M. Silber, H. Riecke und L. Kramer, Physica D **61**, 260 (1992).
[11] I. Rehberg, S. Rasenat, M. de la Torre Juarez, W. Schöpf, F. Hörner, G. Ahlers, and H. Brand, Phys. Rev. Lett **67**, 596 (1991).
[12] I. Rehberg, F. Hörner and H. Hartung, J. Sta. Phys. **64**, 1017 (1991).
[13] M. Dennin, D. S. Cannell and G. Ahlers,, Phys. Rev. E **57**, 638 (1997).
[14] M. Dennin, G. Ahlers, and D. S. Cannell, Phys. Rev. Lett. **77**, 2475 (1996); Science **272**, 388 (1997) U. Bisang and G. Ahlers, Phys. Rev. Lett. **80**, 3061 (1998); Phys. Rev. E **60**, 3910 (1999).
[15] H. Riecke and L. Kramer, Physica D **137**, 124 (2000).
[16] H. Riecke and G.D. Granzow, Phys. Rev. Lett **81**, 333 (1998).
[17] M. Kaiser and W. Pesch, Phys. Rev. E **48**, 4510 (1993).
[18] A. Joets and R. Ribotta, J. Phys. (Paris) **47**, 595 (1986); E. Braun, S. Rasenat, and V. Steinberg, Europhys. Lett. **15**, 597 (1991). S. Nasuno and S. Kai, Europhys. Lett. **14**, 779 (1991); S. Nasuno, O. Sasaki, S. Kai, and W. Zimmermann, Phys. Rev. A. **46**, 4954 (1992).
[19] E. Plaut, W. Decker, A. Rossberg, L. Kramer, W. Pesch, A. Belaidi, and R. Ribotta, Phys. Rev. Lett. **79**, 2376, (1997).
[20] E. Plaut and W. Pesch, Phys. Rev. E, **59**, 1247 (1999).
[21] E. Plaut and R. Ribotta, Europhys. Lett. **38**, 441 (1997).
[22] See the contribution of L. Kramer and W. Pesch in [2].
[23] H. Zhao and L. Kramer, Phys. Rev. E, in press.
[24] H. Richter, A. Buka, and I. Rehberg, in P. Cladis and P. Palffy-Muhoray, editors, *Spatio-temporal patterns in nonequilibrium complex systems*, Santa Fe Institute Studies in the Sciences of Complexity **XXI**, Addison-Wesley, New York, (1994).
[25] H. Zhao, L. Kramer, I. Rehberg, and A. Rudroff. Phys. Rev. Lett. **81**, 4144 (1998).
[26] S. Rudroff, V. Frette and I. Rehberg, Phys. Rev. E **59**, 1814 (1999).
[27] In the calculations of Ref. [19, 20] restabilization of ARs was indeed tested only with respect to ZZ modes.
[28] A.G. Rossberg, PhD thesis, Bayreuth 1998; A.G. Rossberg and L. Kramer, Physica Scripta, **T67** 121 (1996).
[29] A. G. Rossberg, A. Hertrich, L. Kramer, and W. Pesch, Phys. Rev. Lett. **76**, 4729–4732 (1996).
[30] P. Toth, A. Buka, J. Peinke and L. Kramer, Phys. Rev. E **58**(1998).
[31] Y. Hidaka, J.-H. Huh, K. Hayashi, M.I. Tribeski, and S. Kai, Phys. Rev. E **56**, R6256 (1997).
[32] J.-H. Huh and Y. Hidaka, A. G. Rossberg and S. Kai, Phys. Rev. E **61**, 2769 (2000).
[33] A.R. Rossberg, N. Eber, A. Buka and L. Kramer, Phys. Rev. E, **61**, R25 (2000).
[34] A. G. Rossberg and L. Kramer, Physca D **115**, 19 (1998).
[35] A.G. Rossberg, *Three-dimensional pattern formation, multiple homogeneous soft modes, and nonlinear dielectric electroconvection*, preprint, http://arXiv.org/abs/nlin/?0001065 (2000).

[36] M. Scheuring, L. Kramer und J. Peinke, Phys. Rev. **E58**, 2018 (1998).
[37] H. Amm, R. Stannarius, and A.G. Roßberg, Physica D**126**, 171 (1999).
[38] H. Zhao, PhD thesis, Bayreuth 2000.
[39] A.N. Trufanov, L.M. Blinov, and M.I. Barnik, in *Advances in Liquid Crystal Research and Applications*, L. Bata, ed. (Pergamon Press, Oxford-Budapest, 1980), p. 549.
[40] L. Nasta, L. Lupu, and M. Giurgea, Mol. Cryst. Liq. Cryst. **71**, 65 (1981).
[41] W. Weissflog, G. Pelzl H. Kresse, and D. Demus, Crystal Research and Technology **23**, 1259 (1988).
[42] J.-H. Huh and Y. Hidaka, Y. Yusuf, S. Kai, N. Éber, Á. Buka, this proceedings.
[43] M. Treiber, PhD thesis, Universität Bayreuth, (1996).
[44] S. Kai, private communication.
[45] R. Ribotta and G. Durand, J. Phys. Coll. **40**, C3–334 (1979).